CSI-Based Signal Reconstruction for WiFi Localization

Yunbing Hu[1,2](✉), Ao Peng[1], and Shenghong Li[3]

[1] The School of Informatics, Xiamen University, China, Xiamen 361001, China
yunbinghu@stu.xmu.edu.cn
[2] Chongqing College of Electronic Engineering, Chongqing 401331, China
[3] Commonwealth Scientific and Industrial Research Organisation Marsfield, Canberra, NSW 2122, Australia
shenghong.li@csiro.au

Abstract. With the advent of the 5G era, the demand for high-precision wireless positioning continues to grow. However, traditional ranging-based positioning systems are highly susceptible to interferences caused by multipath and none-line-of-sight (LOS) propagation, which can significantly degrade the accuracy of the estimated time-of-arrival (TOA) values. To address this challenge, this paper proposes a Deep neural networks (DNN)-based approach for accurate TOA estimation in indoor environments. Using a complex-values neural network model, the proposed method predicts TOA directly from the frequency domain channel state information (CSI) of wideband WiFi receivers. We also propose an input normalization method based on peak search in the channel impulse response, which improves both the accuracy of TOA estimation and the efficiency of model training. The proposed method was verified experimentally both in an outdoor area of 900 m^2 with 6 anchors and an indoor area of 700 m^2. It is shown that the proposed approach significantly outperforms conventional methods, with 77% of the positioning errors within 0.5 m in the outdoor test and 95% within 1 m. In the indoor test, about 64% of the positioning errors were within 0.5 m, and approximately 80% were within 1 m.

Keywords: Channel state information · IEEE 802.11 signals · Complex value deep neural network

Supported by the National Key Research and Development Project of China (2020YFB1711000), the National Scientific Research Foundation of Chongqing (cstc2019jcyj-msxmX0509), and the Social Scientific Research Foundation of China (19VSZ084), and the National Scientific Research Foundation of Chongqing Municipal Education Commission (KJQN201803110, KJZD-K201903101), and the Social Scientific Research Foundation of Chongqing Municipal Education Commission (20SKGH313), and the National Scientific Research Foundation of Hunan Province Education Commission (18B367), and the Youth Innovation talent Program of Guangxi(AD19245156), and the Teaching Reform Project of Guangxi Normal University(2019XJGZ08).

X. Chen et al. (Eds.): IoTaaS 2023, LNICST 585, pp. 119–128, 2025.
https://doi.org/10.1007/978-3-031-70507-6_10

1 Introduction

Wireless localization is an important research focus because it compensates for the unavailability or inaccuracy of satellite-based positioning systems due to environmental constraints. Applications for wireless indoor and outdoor positioning include underground mining, factory automation, and hospitals. The harsh propagation environment limits the coverage and accuracy of satellite-based localization systems.

In recent years, accurate, reliable and ubiquitous indoor and outdoor localization solutions have been extensively studied based on a range of wireless signals, such as WiFi [1], Bluetooth [2], radar [3], horus [4],Radio Frequency Identification (RFID) [5] , ultra-wideband (UWB) [6], infrared [7], visible light [8], sound [9] , geomagnetic field [10], and so on. However, among these technologies, due to the mass popularity of WiFi systems, the cost of hardware investment is very low, and WiFi based positioning is probably the most popular. Existing wifi devices can be located in a Wifi-based communication system with a firmware upgrade.

The indoor fingerprint recognition system based on CSI has better performance. For example, Liu *et al.* [15] performed CSI amplitude-based localization fingerprint through Cluster-Mapping, which is an adaptive pre-processing system and showed improvement in localization with 98% accuracy with 2-meter localization error. In [16], the authors used only the amplitude of CSI with a deep learning approach and showed 80% localization accuracy with a 2-meter error. In [17], the authors created the collected CSI data as an image and used a deep convolutional neural network to realize localization. The advantage of fingerprint positioning is that while the positioning accuracy is relatively high, it requires laborious survey and measurement of the environment in advance. Once changed, the environment of the position area needs to be measured again, which adversely impacts the commercial versatility of the equipment.

This paper proposes a peak search algorithm based on CSI, which is more accurate than the celebrated MUSIC and ESPRIT algorithms. In practical application, it achieves high positioning accuracy. The main contributions of this work are as follows:

1. We propose a complex neural network model which predicts TOA directly from the frequency domain CSI of wideband WiFi receivers.
2. We propose an input normalization method based on peak search in the channel impulse response, which improves both the accuracy of TOA estimation and the efficiency of model training.
3. The proposed algorithm was experimentally verified on an outdoor positioning system with 6 anchor points covering 900 m^2. The results show that the proposed algorithm has high precision and broad application prospect.

The rest of this article is organized as follows. Section 2 gives the system model, including the structure system and signal structure. Section 3 introduces the data preparation after peak search, and Sect. 4 introduces the neural network structure. Section 5 introduces the evaluation, analysis and experimental verification of the simulation results, and Sect. 5 summarizes the characteristics of the proposed method.

2 System Model

In this paper, we use the wireless ad hoc system for positioning (WASP) [18] developed by the Commonwealth Scientific and Industrial Research Organization (CSIRO) of Australia. The WASP platform features a low-cost, off-the-shelf hardware design that utilizes a bandwidth of 125 MHz for TOA based distance measurement. At the same time, the system has achieved commercial application, and continues to undergo extensive testing and commercial applications in athlete tracking and underground mining.

2.1 System Structure

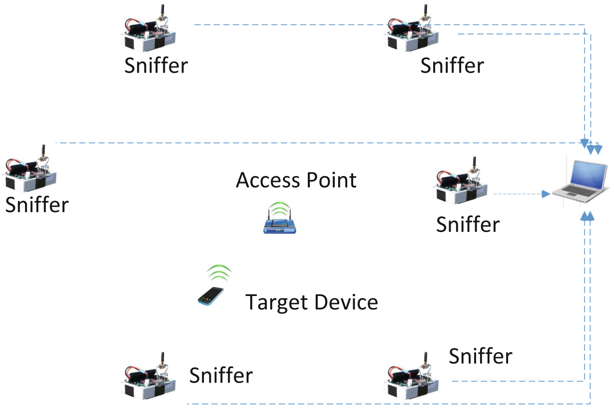

Fig. 1. structure of beacon transmissions in the WASP system.

The localization structure of Fig. 1 is based on a passive WiFi system based on TDOA. The system is composed of 6 custom WiFi sniffers deployed at known locations, a WiFi router, and a laptop computer. The sniffer is used to monitor WiFi network communications, the laptop is used to estimate the target's location from the time stamps collected, and the timestamp monitored by the sniffer is used to calibrate the system hardware delay and provide system clock synchronization.

2.2 Signal Structure

The WASP system adopts WiFi communication technology. WiFi technology based on 802.11a/g/n protocol adopts OFDM system [19]. It includes multiple transmitting antenna at an Access Point (AP) and receiving network card multiple receiving antennas.

Figure 2 shows the architecture of OFDM system, and the architecture of channel estimation and signal detection based on deep learning. At the sending end, the parallel transmission data is converted to serial data. The real and imaginary parts are then converted to the analog domain using a digital-to-analog converter and transmitted out.

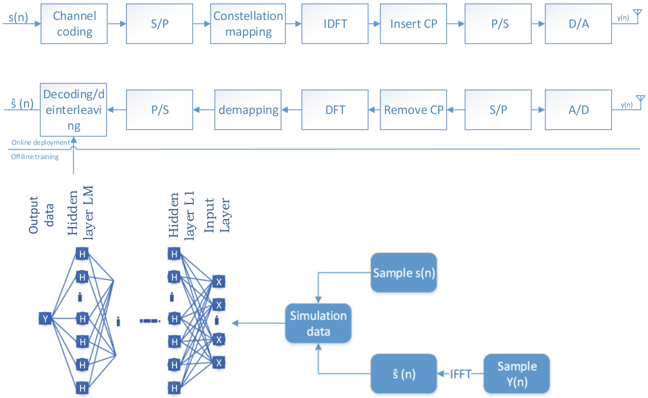

Fig. 2. The system structure of TOA estimation using neural network based on OFDM.

Receiving is the opposite of sending. OFDM enables several subcarriers that are very close to each other to carry the transmitted data to improve the transmission data rate. Each subcarrier transmits data synchronously at the beginning of a frame. Therefore, on the receiving side, using an IEEE 802.11a/g/n compatible wireless network card, a set of CSI can be obtained from each received packet.

3 Deep Learning-Based ToA Estimation

This section presents a method where deep learning is exploited to estimate the received CIR for ToA Estimation. The complex neural network model is trained based on sampling data offline from the WASP system.

3.1 Normalization

Normalization can accelerate the learning speed in the deep network training.

Convertion from Frequency Domain CSI to CIR In practical application, CSI can be characterized by CFR or CIR, and the raw CSI received by the WASP system is CFR in the frequency domain, but the TOA required for positioning is acquired in the time domain. Since CIR is the inverse Fourier transform of CFR [20], it can be expressed as:

$$CIR = IFFT(CSI * W) \tag{1}$$

where W indicates the sampling bandwidth. To do this effectively, the broadband channel is first filled to 1280 samples. Then calculate the IFFT of 1024 points. This improves the sampling accuracy to some extent, making the sampling interval of the impulse response 2.5ns.

Find the Index of the First Significant Peak in the CIR The shape of the leading edge is extracted from the impulse response. The leading edge is resampled to use 25 sample points with a spacing of 1.875ns, such that the peak occurs at sample 25. If the impulse response has multiple peaks, then several leading edges may be extracted. Due to noise and multipath propagation, identifying the leading edge of the impulse response is somewhat involved. Three conditions are used to identify when a peak in the impulse response is due to a received signal, as opposed to being due to noise: (1) The peak must have an amplitude greater than the amplitude of the previous two peaks in the impulse response. (2) The peak must have an amplitude greater than a fixed fraction of the biggest peak amplitude. (3) The peak must have an amplitude greater than the noise floor, which is determined as a multiple of the maximum value of the impulse response in the first 256 samples of the 1024 sample impulse response.

Phase and Amplitude Normalization Phase and amplitude normalization is a linear transformation, which can accelerate the neural network's learning and training speed and improve classification accuracy. Shift the CIR so that the first peak is located at the index center. Figure 3 shows the Phase and amplitude normalization in the CIR. and , the amplitude normalization is adopt to divide by the Amplitude peak value in CIR. this is applied as a normalization step in the machine learning algorithm. It is written as

$$CIR\_norm[N] = CIR[N]/\max(CIR[N]) \tag{2}$$

where $CIR\_norm[N]$ is saved as the normalization of CIR, N represent the number of CIR.

3.2 Training Data Generation

To get good performance from the DL methods, we use the Saleh-Valenzuela channel model to generate 1 million simulated samples of data. The model adopts the time constant of 5ns and 300ns within and between clusters, respectively. The complex amplitude of each path can be expressed as

$$h_k = N(0, \sigma^2) + jN(0, \sigma^2) \tag{3}$$

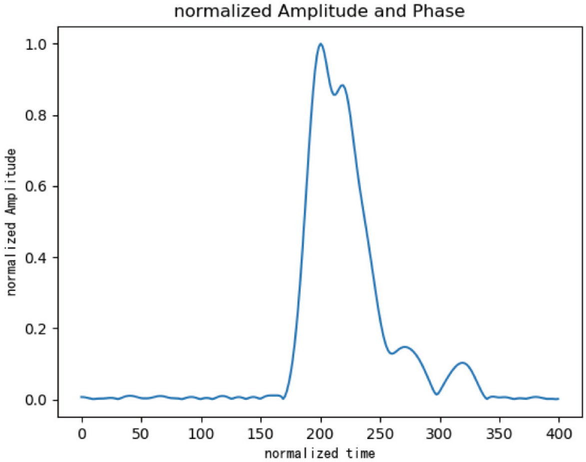

Fig. 3. shift the cir so that the first peak is located at index center.

where $N(\mu, \sigma^2)$ indicates a value drawn from the normal distribution with mean μ and variance σ^2. Equation (3) creates Raleigh amplitude fading. The variance σ^2 undergoes exponential decay both within a cluster and between clusters according to

$$\sigma^2 = e^{-T_l/\Gamma} e^{-\tau_{kl}/\gamma} \tag{4}$$

where T_l is the delay of the l th cluster and $\tau_k l$ is the delay of the k-th path in the l-th cluster. In our simulation, we set $\Gamma = 60$ ns and $\gamma = 20$ ns. We also add noises to give an SNR of 30 dB.

4 Interpretation of the Network

The WASP system based on 802.11a/g/n protocol adopts OFDM system, and the CSI complex H(n) that we can obtain through the WASP system is the $n-$th subcarrier from Target and Sniffer to AP. So given a CSI complex-valued vector $\boldsymbol{h} = \boldsymbol{x} + i\boldsymbol{y}$ [22] , it is represented as

$$\boldsymbol{h} = \begin{bmatrix} \boldsymbol{x} \\ \boldsymbol{y} \end{bmatrix} \tag{5}$$

where is a real component x and a virtual component y. For performing forward propagation of an equivalent traditional real-valued two-dimensional DNN fully connected network, through vector h we construct DNN hidden layer complex filter matrix $W = A + iB$, where the A and B are real matrix, we obtain

$$\boldsymbol{W} * \boldsymbol{h} = (\boldsymbol{A} * \boldsymbol{x} - \boldsymbol{B} * \boldsymbol{y}) + \boldsymbol{i}(\boldsymbol{B}\boldsymbol{x} + \boldsymbol{A}\boldsymbol{y}) \tag{6}$$

If we use matrix represent real and imaginary parts of the CSI, we have

$$\begin{bmatrix} \Re(\boldsymbol{W} * \boldsymbol{h}) \\ \Im(\boldsymbol{W} * \boldsymbol{h}) \end{bmatrix} = \begin{bmatrix} \boldsymbol{A} & -\boldsymbol{B} \\ \boldsymbol{B} & \boldsymbol{A} \end{bmatrix} * \begin{bmatrix} \boldsymbol{x} \\ \boldsymbol{y} \end{bmatrix} \tag{7}$$

To improve the cvDNN fitting ability, we construct a complex bias value $b = m + in$ for cvDNN, where b dimension are the same as and h. Therefore, the linear relationship learned between the output and input of the $n-$th cvDNN neuron z can be expressed as

$$\boldsymbol{z} = \begin{bmatrix} \boldsymbol{A} & -\boldsymbol{B} \\ \boldsymbol{B} & \boldsymbol{A} \end{bmatrix} * \begin{bmatrix} \boldsymbol{x} \\ \boldsymbol{y} \end{bmatrix} + \begin{bmatrix} \boldsymbol{m} \\ \boldsymbol{n} \end{bmatrix} \tag{8}$$

A fully connected feed forward cvDNN consist of an input layer, a complex layer, two real hidden layers (from first to third, each 256 neurons), and an output layer in Fig. 4. The CReLU is used as the activation function of the complex hidden layers, and Parametric Rectified Linear Unit(PReLU) [27] is used as the activation function of the real hidden layers.

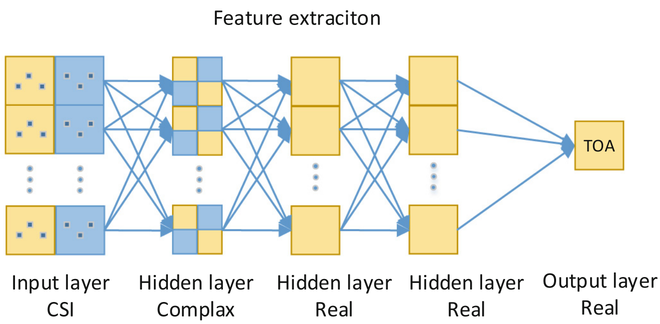

Fig. 4. A diagram illustrating the implementation of a fully connected cvDNN.

Both the complex hidden and the real layer adopted the real Mean Square Error(MSE) loss function. The network is trained in a supervised manner with the MSE loss function, with 0.001 learn rate, 10000 train batch size and 10000 iterations of backpropagation.

5 Experimental Validation

The system was tested under outdoor line-of-sight (LOS) conditions, evaluate its performance. We deployed 6 sniffers around a WiFi network with one access point and one WiFi dongle. A laptop with a WiFi USB dongle was used as the target devices. The topology of the system is shown in Fig. 5.

The laptop communicates with the WiFi router periodically, and the CSI data that the sniffer can sample is used as a reference for hardware delay calibration.

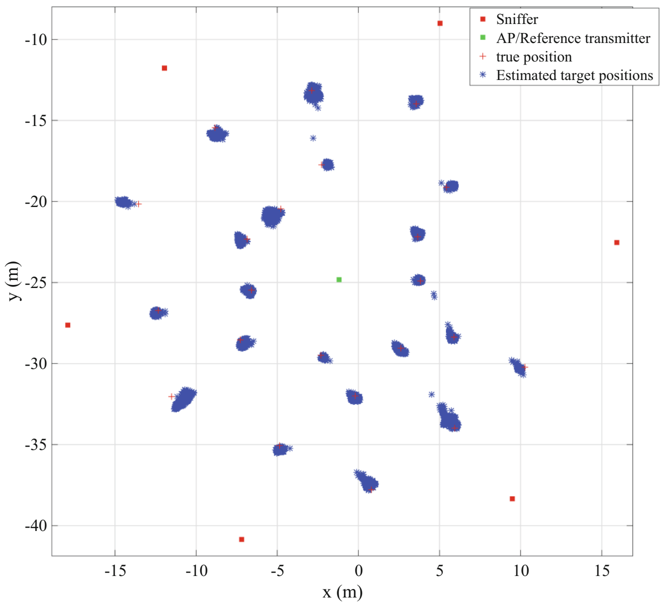

Fig. 5. Positioning effect in outdoor LOS environments.

Fig. 6. Comparison of cumulative distribution function of positioning error in outdoor LOS test.

Figure 6 shows that the TOA estimated by our cvDNN algorithm is better than the positioning accuracy of MUSIC and ESPRIT algorithms. About 80 % of the positioning errors are within the range of 0.5 m.

CONCLUSION

We propose a method to find the CIR peak to obtain the first peak, and then obtain the CIR phase normalization, thereby improving the performance of neural network regression, and propose a cvDNN method suitable for CSI. The experimental verification was carried out on an outdoor positioning system covering an area of 900 square meters and 22 nodes. The results show that the proposed algorithm has higher localization accuracy, and it has greater market application potential than fingerprint legal bit because it does not need to collect data in the experiment site in advance.

References

1. Yang, C., Shao, H.-R.: WiFi-based indoor positioning. IEEE Commun. Mag. **53**(3), 150–157 (2015)
2. Kriz, P., Maly, F., Kozel, T.: Improving indoor localization using Bluetooth low energy beacons. Mobile Inf. Syst. **2016**, 2083094 (2016)
3. Bahl, P., Padmanabhan, V.N.: Radar: an in-building RF-based user location and tracking system. In Proc, pp. 775–784. Tel Aviv, Israel, (2000), IEEE INFOCOM
4. Youssef, M., Agrawala, A.: The Horus WLAN location determination system. In: Proceeding Seattle, WA, USA ACM MobiSys. pp. 205–218 (2005)
5. Zhou, Z., Shangguan, L., Zheng, X., Yang, L., Liu, Y.: Design and implementation of an RFID-based customer shopping behavior mining system. IEEE/ACM Trans. Netw. **25**(4), 2405–2418 (2017)
6. B. Kempke, P. Pannuto, B. Campbell, and P. Dutta, "SurePoint: Exploiting ultra wideband flooding and diversity to provide robust, scalable, high-fidelity indoor localization. In: Proceedings 14th ACM Conference Embedded Network Sensor Syst. (CD-ROM), pp. 137-149 (2016)
7. Hauschildt, D., Kirchhof, N.: Advances in thermal infrared localization: challenges and solutions. In: Proceedings IEEE International Conference Indoor Positioning Indoor Navigation. (IPIN). pp. 1–8 (2010)
8. Pathak, P.H., Feng, X., Hu, P., Mohapatra, P.: Visible light communication, networking, and sensing: a survey, potential and challenges. IEEE Commun. Surveys Tuts. **17**(4), 2047–2077 (2015)
9. Moutinho, J.N., Araújo, R.E., Freitas, D.: Indoor localization with audible sound-Towards practical implementation. Pervas. Mobile Comput. **29**, 1–16 (2016)
10. Shu, Y., Bo, C., Shen, G., Zhao, C., Li, L., Zhao, F.: Magicol: Indoor localization using pervasive magnetic field and opportunistic WiFi sensing. IEEE J. Sel. Areas Commun. **33**(7), 1443–1457 (2015)
11. Yang, Z., Zhou, Z., Liu, Y.: From RSSI to CSI: indoor localization via channel response. ACM Comput. Surv. **46**(2), 25–32 (2013)
12. Bahl, P., Padmanabhan, V.N.: RADAR: An in-building RF-based user location and tracking system[C]// INFOCOM 2000. Nineteenth Annual Joint Conference of the IEEE Computer and Communications Societies. Proceedings. IEEE. IEEE (2000)
13. Gu, Yang, et al.: Semi-supervised deep extreme learning machine for WiFi based localization. Neurocomputing **166**(7), 282–293 (2015)

14. Halperin, D., Hu, W., Sheth, A., Wetherall, D.: Tool release: Gathering 802.11n traces with channel state information. ACM SIGCOMM Comput. Commun. Rev. **41**(1), 53–53 (2011)
15. Liu, Wen, et al.: C-Map: hyper-resolution adaptive preprocessing system for csi amplitude-based fingerprint localization. IEEE Access **99**, 1–10 (2019)
16. Wang, Xuyu, et al.: CSI-based fingerprinting for indoor localization: a deep learning approach. IEEE Trans. Vehi. Technol. **66**(1), 763–776 (2016)
17. Wang, Xuyu, Wang, X., Mao, S.: Deep convolutional neural networks for indoor localization with CSI images. IEEE Trans. Netw. Sci. Eng. **7**(1), 316 (2018)
18. Li, Shenghong, Hedley, M., Collings, I.B.: New efficient indoor cooperative localization algorithm with empirical ranging error model. IEEE J. Select. Areas Commun. **33**(7), 1407–1417 (2015)
19. Cheng, Peng, et al.: Sparse blind carrier-frequency offset estimation for OFDMA uplink. IEEE Trans. Commun. **64**(12), 5254–5265 (2016)
20. Zhou, Z., Wu, C., Yang, Z., Liu, Y.: Sensorless sensing with WiFi. Tsinghua Sci. Technol. **20**(1), 1–6 (2015)
21. K. Pahlavan, A. Levesque, "Wireless information network s", 2^{nd}ed. chapter 6, Wiley 2005
22. Trabelsi, Chiheb, et al. Deep Complex Networks. (2017)
23. Li, Shenghong, et al. TDOA-based passive localization of standard WiFi devices. Ubiquitous Positioning, Indoor Navigation and Location-Based Services 0
24. Bao, Qiao, et al.: Research on single frequency component based MUSIC algorithm for impact localization." International Conference on Noise & Fluctuations IEEE, (2015)
25. Li, Shenghong, et al.: TDOA-based passive localization of standard WiFi devices. 2018 Ubiquitous Positioning, Indoor Navigation and Location-Based Services (UPINLBS) (2018)
26. Li, Shenghong, et al.: TDOA-based localization for semi-static targets in NLOS environments. IEEE Wirel. Commun. Lett. **4**(5), 1–1 (2015)
27. He, K. , et al.: Delving Deep into Rectifiers: surpassing human-level performance on imagenet classification. CVPR IEEE Computer Society (2015)
28. Shang, W., et al.: Understanding and improving convolutional neural networks via concatenated rectified linear units. JMLR (2016)